JPE 2-2-3

Sensorless Control of the Synchronous Reluctance Machine

A. Kilthau and J. M. Pacas*

Institute of Power Electronics and Electrical Drives, University of Siegen, Germany

ABSTRACT

The paper deals with the control of the synchronous reluctance machine without position sensor. A method for the computation of the transformation angle out of terminal voltages and currents is presented. The injection of test signals allows operation at zero speed. Fundamental for this control scheme is the exact modelling of the machine, where especially the saturable inductances are of central interest. The accuracy of the angle estimation method over the whole operating range including field-weakening is discussed in detail. The implementation of the angle estimation method in a rotor-oriented control scheme and practical results are demonstrated.

Key Words: Electrical machines, Synchronous machines, Reluctance motors, Servomotors, Modeling, Variable speed drives

1. Introduction

It is well known that the synchronous reluctance machine is an alternative to permanent magnet synchronous and induction machines. Compared with permanent magnet synchronous machines it has lower costs and can function at very high speed because of the easier field weakening capability and the rugged rotor. If compared to asynchronous machines it has theoretically no rotor losses and a comparable torque density depending on the design of the machine.

On the other hand, the complexity of the dynamic equations of the synchronous reluctance machine is increased due to the different magnetic characteristics in the axis d and q. As a result, the control of synchronous reluctance machines faces some special problems different to other AC machines.

The vector control of the synchronous reluctance machine leads to structures where the saturable inductances L_d and L_q are of central interest. Particularly in sensorless control schemes the model of the machine and its parameters should describe the system as good as possible. In the case of the synchronous reluctance machine the obvious sensorless control method is to evaluate the magnetic unbalance of the rotor. The presented method is confirmed by experiment. For the experimental work a commercial available machine was used.

2. Mathematical Model

The synchronous reluctance machine can be described by the following well known set of equations in the d-q-reference frame:

$$u_d = R_s i_d + \frac{d\psi_d}{dt} - \omega\psi_q \ , \quad \psi_d = L_d i_d$$
$$u_q = R_s i_q + \frac{d\psi_q}{dt} + \omega\psi_d \ , \quad \psi_q = L_q i_q \tag{1}$$

$$M_i = \frac{3}{2} p\left(L_d - L_q\right) i_d i_q \tag{2}$$

Manuscript received January 8, 2002; revised April 25, 2002.
Corresponding Author: pacas@lea.e-technik.uni-siegen.de, Tel: +49-271-740-4671, Fax: +49-271-740-2777

$$J\frac{d\omega_{mech}}{dt}=M_i-M_L \quad , \quad \omega_{mech}=\frac{\omega}{p} \tag{3}$$

The iron saturation can be easily considered by assuming the inductances dependent on the currents. Since the cross coupling is taken into account each inductance is dependent both on i_d and i_q:

$$\begin{aligned}\psi_d &= L_d(i_d,i_q)\cdot i_d\\ \psi_q &= L_q(i_d,i_q)\cdot i_q\end{aligned} \tag{4}$$

Hence by using the derivation rules (1) becomes:

$$\begin{aligned}u_d &= R_s i_d + L_{dt}\frac{di_d}{dt}+i_d\left(\frac{\partial L_d}{\partial i_q}\frac{di_q}{dt}\right)-\omega L_q i_q\\ u_q &= R_s i_q + L_{qt}\frac{di_q}{dt}+i_q\left(\frac{\partial L_q}{\partial i_d}\frac{di_d}{dt}\right)+\omega L_d i_d\end{aligned} \tag{5}$$

with:

$$\begin{aligned}L_{dt} &= L_d + i_d\frac{\partial L_d}{\partial i_d}\\ L_{qt} &= L_q + i_q\frac{\partial L_q}{\partial i_q}\end{aligned} \tag{6}$$

Equation (5) and (6) can be interpreted as follows:
The inductances L_d and L_q determine in steady-state operation the mean value of the induced voltage and the torque. The transient inductances L_{dt} and L_{qt} affect the changes of current and flux and an additional term dependent on the grade of cross coupling creates a transient disturbance voltage.

Fig. 1 shows the measured machine parameters. The inductances are the result of a current decay test [1].

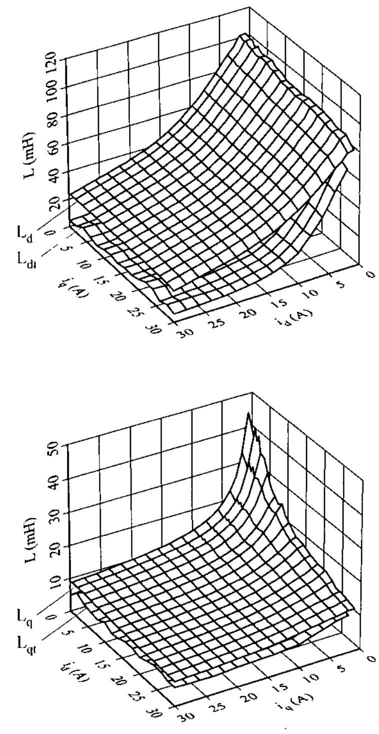

Fig. 1. Stationary inductances L_d, L_q and transient inductances L_{dt}, L_{qt} measured with a current decay test.

3. Estimation of the Transformation Angle

Aim of the presented sensorless control scheme is to calculate the transformation angle out of the terminal voltages and currents. The basic requirement for this kind of doing is an accurate machine model, provided with the measurements in [1]. The estimation of the rotor position angle γ will be carried out by using the developed non-linear and deterministic model and a test signal in the lower speed range.

$$\begin{aligned}
a_d &= \frac{1}{\sqrt{3}}\cdot\left[\left(R_s+\sqrt{3}\,\omega\left(L_q-L_{dt}\right)-\omega i_d\frac{\partial L_d}{\partial i_q}\right)\cdot i_U+2\left(R_s-\omega i_d\frac{\partial L_d}{\partial i_q}\right)\cdot i_V+\left(L_{dt}-\sqrt{3}\,i_d\frac{\partial L_d}{\partial i_q}\right)\cdot\frac{di_U}{dt}+2L_{dt}\cdot\frac{di_V}{dt}-u_U-2u_V\right]\\
b_d &= \frac{1}{\sqrt{3}}\cdot\left[\left(\sqrt{3}\,R_s-\omega\left(L_q-L_{dt}\right)-\sqrt{3}\,\omega i_d\frac{\partial L_d}{\partial i_q}\right)\cdot i_U-2\omega\left(L_q-L_{dt}\right)\cdot i_V+\left(\sqrt{3}\,L_{dt}+i_d\frac{\partial L_d}{\partial i_q}\right)\cdot\frac{di_U}{dt}+2i_d\frac{\partial L_d}{\partial i_q}\cdot\frac{di_V}{dt}-\sqrt{3}\,u_U\right]\\
a_q &= \frac{-1}{\sqrt{3}}\cdot\left[\left(\sqrt{3}\,R_s-\omega\left(L_d-L_{qt}\right)+\sqrt{3}\,\omega i_q\frac{\partial L_q}{\partial i_d}\right)\cdot i_U-2\omega\left(L_d-L_{qt}\right)\cdot i_V+\left(\sqrt{3}\,L_{qt}-i_q\frac{\partial L_q}{\partial i_d}\right)\cdot\frac{di_U}{dt}-2i_q\frac{\partial L_q}{\partial i_d}\cdot\frac{di_V}{dt}-\sqrt{3}\,u_U\right]\\
b_q &= \frac{1}{\sqrt{3}}\cdot\left[\left(R_s+\sqrt{3}\,\omega\left(L_d-L_{qt}\right)+\omega i_q\frac{\partial L_q}{\partial i_d}\right)\cdot i_U+2\left(R_s+\omega i_q\frac{\partial L_q}{\partial i_d}\right)\cdot i_V+\left(L_{qt}+\sqrt{3}\,i_q\frac{\partial L_q}{\partial i_d}\right)\cdot\frac{di_U}{dt}+2L_{qt}\cdot\frac{di_V}{dt}-u_U-2u_V\right]
\end{aligned} \tag{8}$$

Equation (5) can be expressed in terms of the measured currents and voltages (U, V):

$$a_d \cdot \sin(\gamma_e) + b_d \cdot \cos(\gamma_e) = 0$$
$$a_q \cdot \sin(\gamma_e) + b_q \cdot \cos(\gamma_e) = 0 \qquad (7)$$

where, a_d, a_q, b_d and b_q are the coefficients according to (8) and γ_e is the rotor position angle to be estimated.

The currents in the terms $i_d \cdot \partial L_d/\partial i_q$ and $i_q \cdot \partial L_q/\partial i_d$ are not converted to UVW-coordinates because otherwise the equations cannot be solved for γe. For the machine parameters L_d, L_q, L_{dt}, L_{qt} the respective values calculated with the currents i_d, i_q of the previous control interval are used.

After the calculation of the coefficients a_d, b_d, a_q and b_q out of the model parameters of the previous control interval and the voltages u_U, u_V and currents i_U, i_V of the actual control interval (7) can be solved for γ_e:

$$\gamma_{e1} = \begin{cases} -a\tan\left(\dfrac{b_{d,q}}{a_{d,q}}\right) & \text{for} \quad a_{d,q} \geq 0 \\ -a\tan\left(\dfrac{b_{d,q}}{a_{d,q}}\right) + \pi & \text{for} \quad a_{d,q} < 0 \end{cases} \qquad (9)$$

$$\gamma_{e2} = \gamma_{e1} + \pi$$

Equation (7) has two possible solutions γ_{e1} and γ_{e2}. In the case of the synchronous reluctance machine both solutions are valid because the synchronous reluctance machine has no rotor winding or permanent magnets. However it must be ensured that the estimation algorithm uses only one of these two solutions. A displacement of γ_e by 180 degrees would cause a sign reversal of voltages and currents.

The meaning of the coefficients ad, a_q, b_d and b_q can be illustrated by applying the transformation rules once again to (8). This leads to the more transparent relationships:

$$a_d = -c_d \cdot cos(\gamma_e) \qquad a_q = c_q \cdot cos(\gamma_e)$$
$$b_d = c_d \cdot sin(\gamma_e) \qquad b_q = -c_q \cdot sin(\gamma_e) \qquad (10)$$

with

$$c_d = \omega \ \left(L_d - L_q\right) \cdot i_d - \left(L_{dt} - L_{qt}\right) \cdot \frac{di_q}{dt} + \left(i_d \frac{\partial L_d}{\partial i_q} + i_q \frac{\partial L_q}{\partial i_d}\right) \cdot \frac{di_d}{dt}$$

$$c_q = \omega \ \left(L_d - L_q\right) \cdot i_q + \left(L_{dt} - L_{qt}\right) \cdot \frac{di_d}{dt} + \left(i_d \frac{\partial L_d}{\partial i_q} + i_q \frac{\partial L_q}{\partial i_d}\right) \cdot \frac{di_q}{dt}$$

(11)

For a good quality of angle estimation the coefficients c_d and c_q must be significant greater than zero. The first term in c_d and c_q represents the induced EMF and can be used for angle estimation at higher speed. At standstill the angle can be estimated using the second term. In this case di/dt can be increased by injecting a superimposed alternating voltage. The third term is caused by cross saturation effects. It will be shown that the consideration of this term increases the accuracy of the estimation.

Fig. 2 shows the charts of c_d and c_q when there is no superimposed voltage. These considerations are necessary to select the regions where the angle is calculated out of ad, b_d or out of a_q, b_q. It can be seen that at no-load the angle must be estimated using ad and b_d because c_q is zero. At high load and high speed the estimation of γ_e using a_q and b_q is expected to give the better results because c_q is greater than c_d.

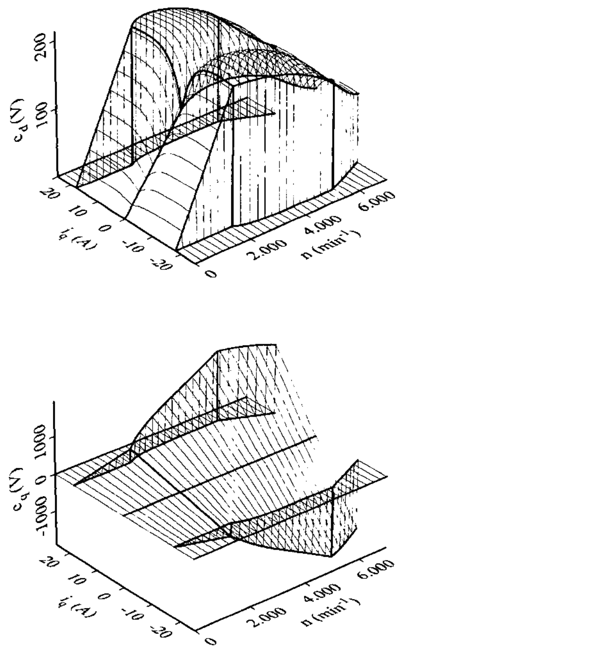

Fig. 2. Magnitude of c_d and c_q without superimposed voltage.

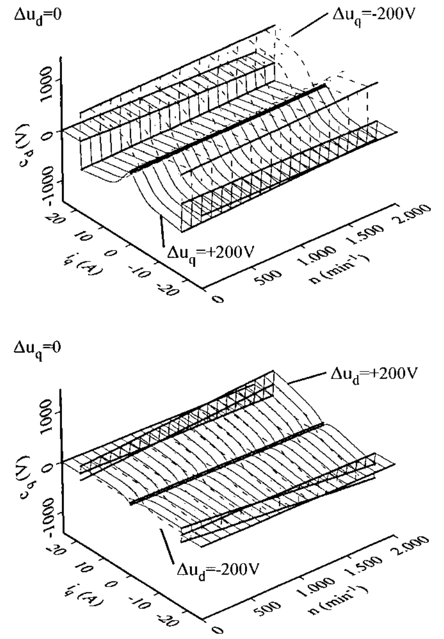

Fig. 3. Magnitude of c_d and c_q with superimposed voltage in base speed range.

3.1 Angle Estimation at Slow Speed

At zero speed and di/dt=0 both cd and c_q in Fig. 2 become zero. According to (11) c_d becomes ≠0 at ω=0 when creating a di_q/dt and c_q becomes ≠0 at ω=0 when creating a di_d/dt. This can be achieved by injecting a rectangular voltage ±Δu in the required axis. The period of the superimposed voltage is selected to be 600μs. The currents are measured at the beginning of each control interval of 150μs, so di/dt is calculated out of the difference between current measurements of a 300μs-interval. The amplitude of the superimposed voltage is set to Δu=±200V.

Using (5) di_d/dt and di_q/dt can be expressed as functions of Δu. Fig. 3 shows the resulting characteristics cd and cq with a superimposed voltage Δu in the d- or q-axis. Because L_{dt} is greater than L_{qt} the magnitude of di_d/dt and c_q is smaller than the magnitude of di_q/dt and c_d. Also c_q becomes zero at certain values i_q<0. Therefore the angle should be estimated using a_d, b_d with injection of Δu in the q-axis. An additional problem is the magnitude of c_d at i_q=0. The reason is that the difference L_{dt}-L_{qt} in (11) at the currents i_d=10A and i_q=0 is nearly zero. The entire dependence of c_d on i_d and i_q at standstill is shown in Fig. 4. Because L_{dt} increases as id decreases the current id

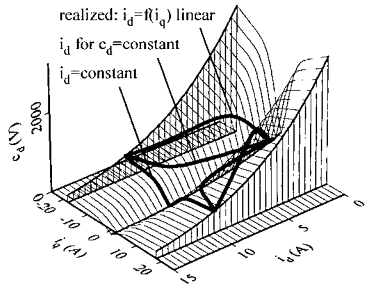

Fig. 4. Magnitude of c_d as a function of i_d, i_q at standstill and with superimposed voltage Δu_q=-200V.

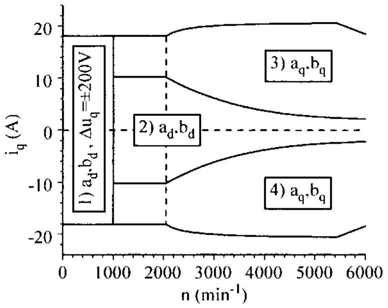

Fig. 5. Regions where the angle γ is calculated out of a_d, b_d or a_q, b_q.

must be decreased at small values of i_q in order to get a value of c_d significantly greater than zero, see Fig. 6.

3.2 Estimation Strategy

The aim of the following considerations is to obtain a magnitude of c_d or c_q as high as possible in each operation point. For this purpose the n-i_q-plane is divided into 4 sections, see Fig. 5. The resulting magnitudes of c_d and c_q are shown in Fig. 8.

1) In the range of -1000min^{-1}<n<1000min^{-1} a rectangular voltage of ±200V is injected in the q-axis. At speed higher than 1000min^{-1} the superimposed voltage would reach the voltage limit of the inverter. The selected reduction strategy of i_d in this region shows Fig. 6.

2)-4) For speed above 1000min^{-1} the method which results in the highest amplitude of c_d or c_q is selected.

In this way the magnitudes of c_d and c_q are never equal to zero, see Fig. 8. Additionally to the considerations above it must be selected among the two possible solutions γ_{e1} and γ_{e2} in (9):

$$\gamma_e = \begin{cases} \gamma_{e1} & \text{for } c_d < 0, \quad -c_q < 0 \\ \gamma_{e2} & \text{for } c_d > 0, \quad -c_q > 0 \end{cases} \tag{12}$$

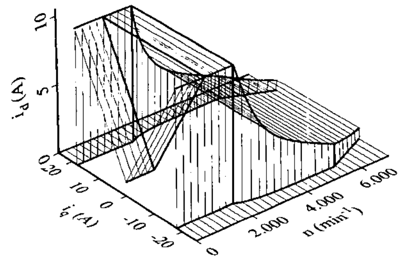

Fig. 6. Complete i_d-characteristic with reduction of i_d when applying an additional voltage at slow speed.

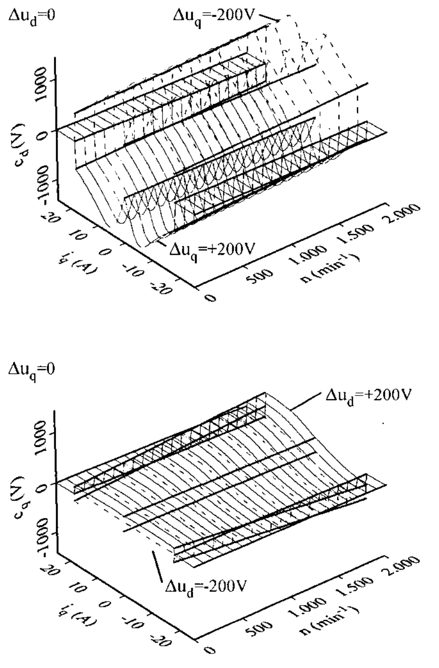

Fig. 7. Magnitude of c_d and c_q with linear reduction of i_d=f(i_q) in base speed range like it is shown Fig. 6.

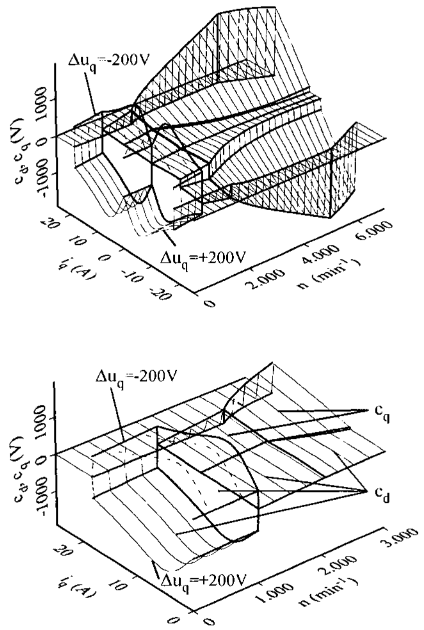

Fig. 8. Resulting magnitudes of c_d and c_q.

3.3 Speed and position observer

Using the described method the rotor angle can be estimated with sufficient accuracy. Still there are problems at dynamic variations of the currents. In this case the stationary characteristics of c_d and c_q shown in Fig. 8 are not valid because of the term di/dt in (11), and therefore some estimated values γe become incorrect at small values of c_d or c_q. It is also impossible to get a speed value with sufficient accuracy by derivation of the estimated angle due to the noise in this signal. The described problems can be solved by using an observer for the mechanical subsystem of the machine.

The general form of a state-space model is:

$$\begin{aligned} \frac{d\mathbf{x}(t)}{dt} &= \mathbf{A}\cdot\mathbf{x}(t)+\mathbf{B}\cdot\mathbf{u}(t)+\mathbf{E}\cdot\mathbf{z}(t) \\ \mathbf{y}(t) &= \mathbf{C}\cdot\mathbf{x}(t)+\mathbf{D}\cdot\mathbf{u}(t) \end{aligned} \tag{13}$$

By applying the equations of the mechanical subsystem of the machine to (13) the state-space model becomes:

$$\begin{aligned} \frac{d}{dt}\begin{pmatrix}\omega(t)\\ \gamma(t)\end{pmatrix} &= \begin{pmatrix}0 & 0\\ 1 & 0\end{pmatrix}\cdot\begin{pmatrix}\omega(t)\\ \gamma(t)\end{pmatrix}+\begin{pmatrix}\frac{p}{J}\\ 0\end{pmatrix}\cdot M_i(t)+\begin{pmatrix}-\frac{p}{J}\\ 0\end{pmatrix}\cdot M_L(t) \\ \gamma(t) &= \begin{pmatrix}0 & 1\end{pmatrix}\cdot\begin{pmatrix}\omega(t)\\ \gamma(t)\end{pmatrix}+0\cdot M_i(t) \end{aligned} \tag{14}$$

The disturbance variable M_L is unknown. Still it is possible to consider the disturbance variable if the time characteristic of the disturbance is basically known. Here the load torque is assumed to be constant. Therefore the disturbance model is:

$$\frac{d}{dt}M_L = 0 \tag{15}$$

The observer structure can be derived out of (14) and (15) in a formal way (see Fig. 9 (a)). The dynamic of the observer is given by the feedback coefficients l_1 and l_2.

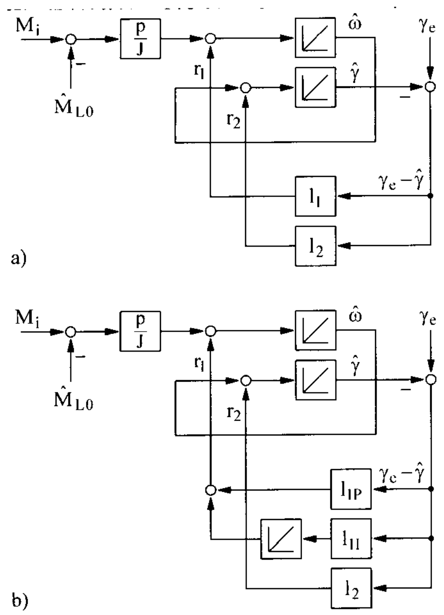

Fig. 9. Structure of the observer with: a) P- and b) PI-feedback.

In the case of $M_L \neq \hat{M}_{L0}$ the difference between reality and model is compensated by the feedback variable r_1 in Fig. 9 (a). As a consequence there is a stationary error in $\hat{\gamma}$ and $\hat{\omega}$ dependent on M_L, l_1 and l_2. The stationary error in $\hat{\omega}$ can be eliminated by using the signal $d\hat{\gamma}/dt$ as speed variable, but then the noise of the estimated angle γ_e deteriorates the quality of the estimated speed.

These disadvantages are eliminated by using the observer structure in Fig. 9 (b). With the integrator in the feedback loop the stationary error of $\hat{\gamma}$ and $\hat{\omega}$ becomes zero.

4. Experimental results

The control scheme has been realized in the laboratory. The simplified control scheme is shown in Fig. 10, see also [2]. The DC link voltage of the inverter is controlled to a fix value of 670V. The inverter uses a space vector PWM, the switching frequency is 3,3kHz and the sampling frequency is 6,6kHz. The inductance characteristics are implemented by using polynomials with an order of 6 ($L_d(i_d)$) and 9 ($L_q(i_q)$) and with a linear dependence $L_d(i_q)$ and $L_q(i_d)$.

First the machine is operated with an angular sensor for the control. In Fig. 11 and Fig. 12 the simulated and measured transient error of the estimated angle γ_e is examined by the example of a positive and negative step of i_q. The resulting magnitude $|c|$ is calculated out of the actually used coefficients a and b according to:

$$|c| = \sqrt{a^2 + b^2} \tag{16}$$

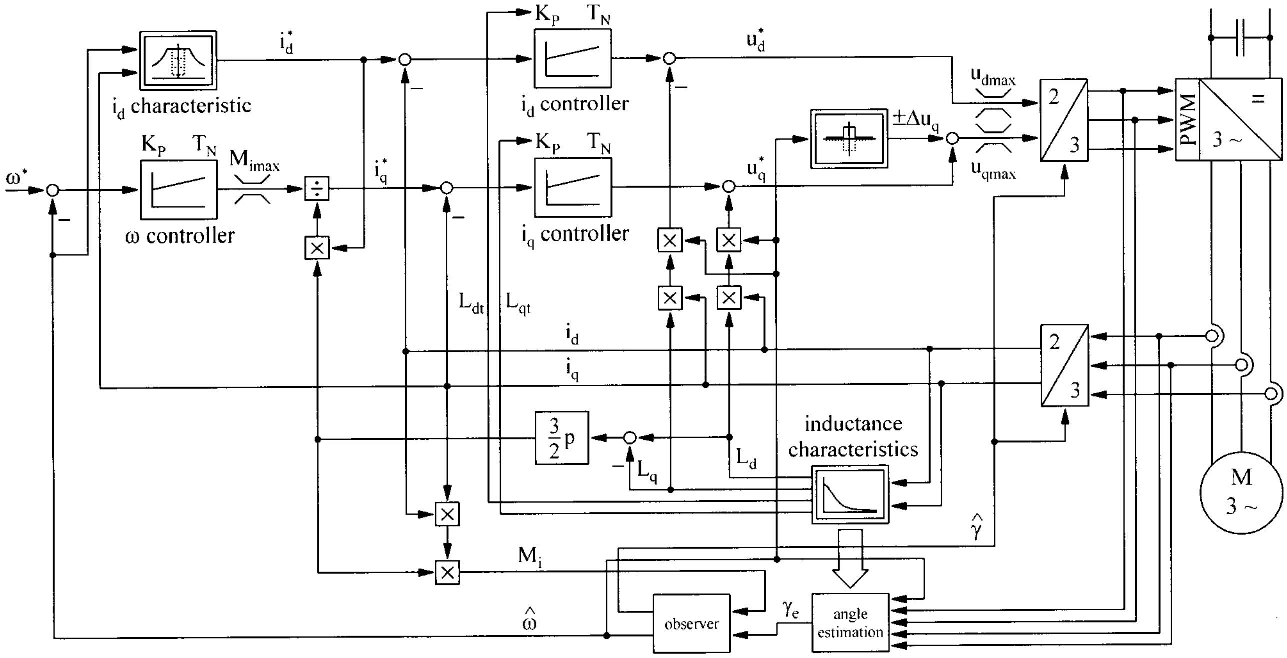

Fig. 10. Control scheme of the synchronous reluctance machine.

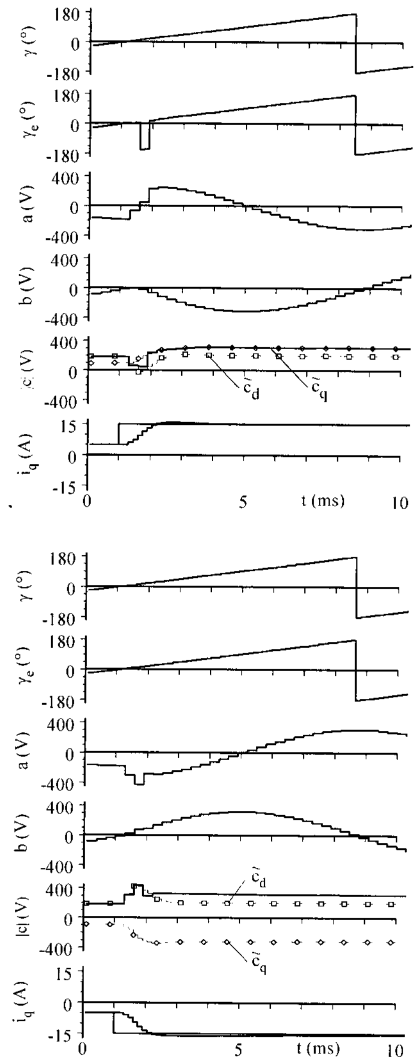

Fig. 11. Simulated positive and negative step responses of i_q at n=2000min^{-1}.

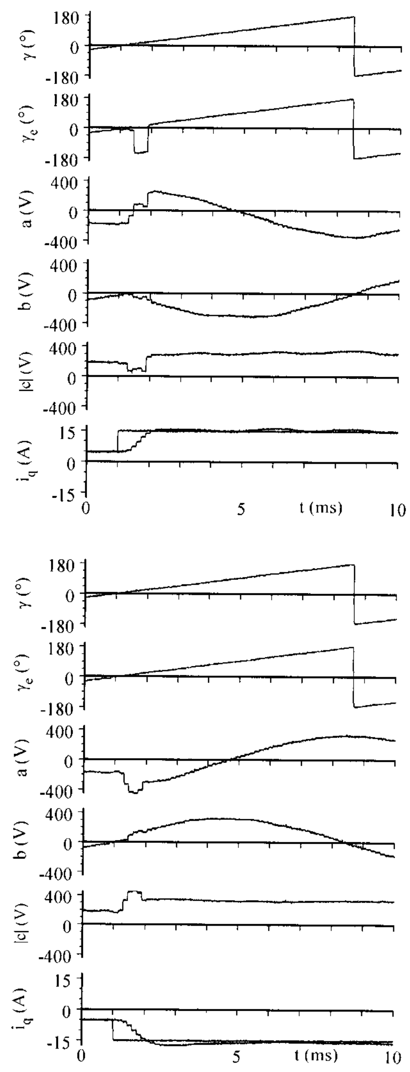

Fig. 12. Measured positive and negative step responses of i_q at n=2000min^{-1}.

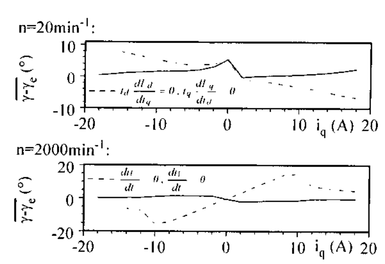

Fig. 13. Average difference between measured and estimated angle.

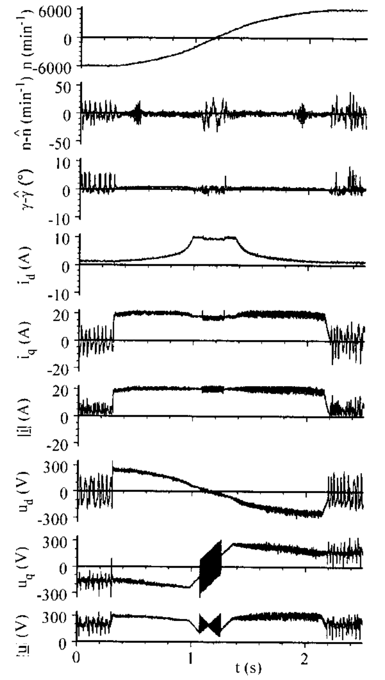

Fig. 14. Measured control variables during speed reversal with a load inertia of $11\cdot10^{-3}$ kgm^2.

In Fig. 11 there are also shown the magnitudes $\tilde{c}_d$ and $\tilde{c}_q$ calculated out of the control variables according to (11). At the positive step of i_q here c_d becomes negative because of the high value of di_q/dt in (11). Because cd is assumed to be positive in this operating point (see Fig. 8), the estimated angle is not corrected according to (12) and so there is a temporary change in γ_e by 180°. At a negative step of iq this problem does not arise because cd remains positive.

A step of the transformation angle by 180° is not tolerable. Even when using the observer a noisy input value γ_e would reduce the quality of the observed transformation angle $\hat{\gamma}$. So this problem has been solved by an additional plausibility check and correction of the estimated angle γe by 180° with $\hat{\gamma}$ as comparison value. Now the measured angle γ and the estimated angle γ_e are compared in steady-state operation in order to verify the estimation algorithm. The average difference ($\gamma-\gamma_e$) at n=20min^{-1} and n=2000min^{-1} shows Fig. 13. Normally the error is less than 2 degrees, only at i_q=0 and with superimposed voltage (n=20min^{-1}) the error increases. The dotted curves in Fig. 13 show the error when the di/dt- or the cross saturation-term in (8) is neglected.

Thus it is proved that consideration of the cross saturation

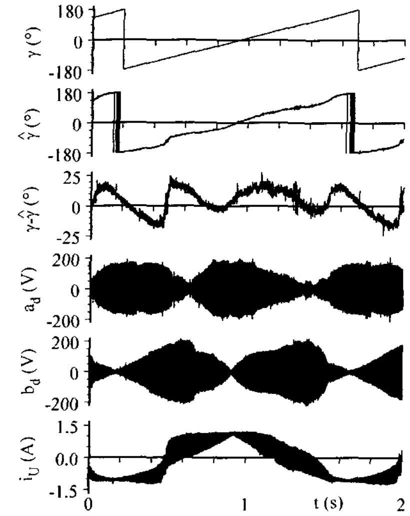

Fig. 15. Control variables at $n=20min^{-1}$, $i_q=0A$.

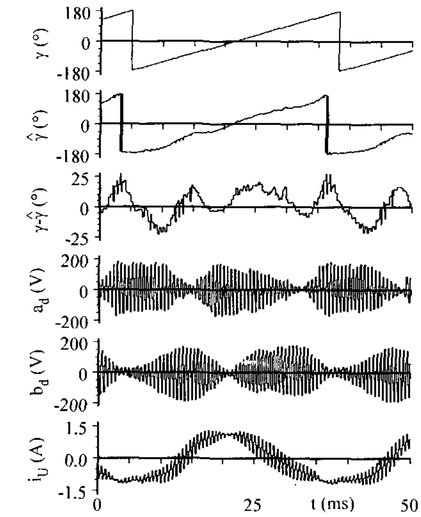

Fig. 16. Control variables at $n=900$ min^{-1}, $i_q=0A$.

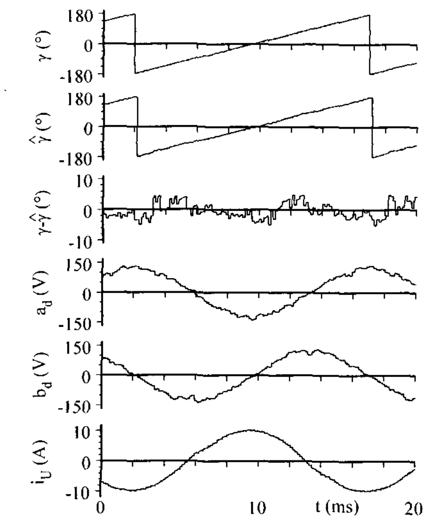

Fig. 17. Control variables at $n=2000$ min^{-1}, $i_q=0A$.

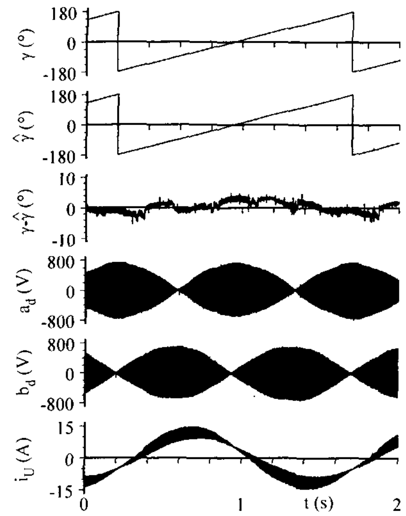

Fig. 18. Control variables at $n=20$ min^{-1}, $i_q=10A$.

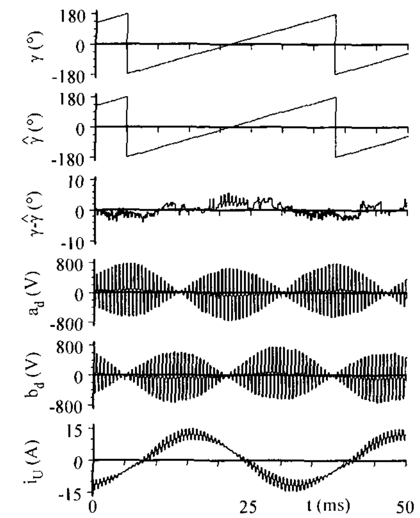

Fig. 19. Control variables at $n=900$ min^{-1}, $i_q=10A$.

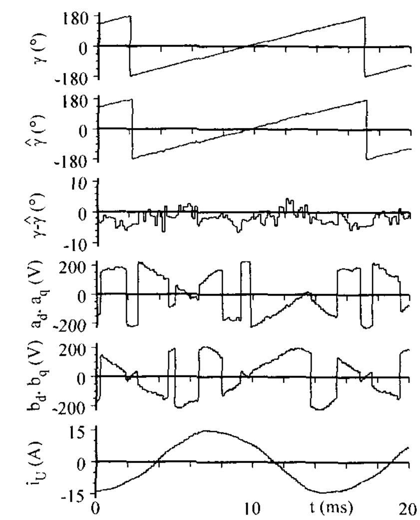

Fig. 20. Control variables at $n=2000$ min^{-1}, $i_q=10A$.

increases the estimation accuracy.

In the next step the machine is controlled according to Fig. 10 using the observed variables $\hat{\gamma}$ and $\hat{\omega}$. Fig. 14 shows a speed reversal from –6000 to +6000min-1 and the errors of the observed speed and position.

In Fig. 15 up to Fig. 20 some measured waveforms in different operating points are given. The greatest error $\gamma-\hat{\gamma}$ is at no load and with superimposed voltage. At n=2000min-1 and i_q=10A the calculation of γ_e switches between using ad, b_d and using aq, b_q.

5. Conclusion

This paper presents a sensorless control scheme for the synchronous reluctance machine. The calculation method uses one measured value of the currents per control cycle, so additional measurements are not necessary. Using the presented model of the machine, the transformation angle can be estimated out of the terminal voltages and currents over the whole speed and load range by means of a non-linear deterministic model. This investigation is a basic work regarding the use of the synchronous reluctance machine in speed-controlled low-cost electrical drives.

6. Nomenclature

d, q: direct and quadrature axis
U, V, W: stator phases
^: observed values *: reference values
u: voltage i: current
ψ: flux linkage R_s: stator resistance
L_d, L_q: stationary inductances
L_{dt}, L_{qt}: transient inductances
ω: angular frequency n: rotational speed
p: number of the pairs of poles
M_i: air-gap torque M_L: load torque
J: inertia γ: rotor angle
γ_e: estimated rotor angle
a, b: coefficients for angle estimation
c: magnitude of a and b
Δu_d, Δu_q: amplitude of the test signal at low speed

Machine data

ABB servomotors, type 2E5.7

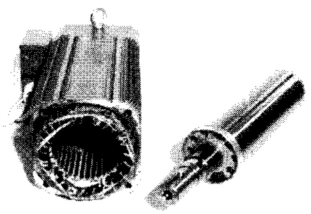

rated torque	M_r=27 Nm
rated current	I_r=14,6 A
number of poles	p=4
rotor inertia	$J=7{,}041\cdot10^{-3}\cdot\text{kgm}^2$
stator resistance	R_S=0,34 Ω

References

[1] Kilthau A. and Pacas, J.M., "Measurement of the Parameters of the Synchronous Reluctance Machine including Cross Saturation", *EPE Graz*, Aug. 2001.

[2] Kilthau, A. and Pacas, J.M., "Control of Synchronous Reluctance Machines", *PCIM Nürnberg*, June 2001.

[3] Vagati, A., Pastorelli, M., Scapino, F., and Franceschini, G., "Impact of cross saturation in synchronous reluctance motors of the transverse-laminated type", *IEEE Trans. on Industry Applications*, Vol. 36, No. 4, pp. 1039~1046, July/ Aug. 2000.

[4] Kang, S.J., Kim, J.M., and Sul, S.K., "Position sensorless control of synchronous reluctance motor using high frequency current injection", *IEEE Trans. on Energy Conversion*, Vol. 14, pp. 1271~1275, Dec.1999.

[5] Jovanovic, M.G., Betz, R.E., and Platt, D., "Sensorless vector controller for a synchronous reluctance motor", *IEEE Trans. on Industry Applications*, Vol. 34, No. 2, pp. 346~353, March/April 1998.

[6] Chomat, M. and McCulloch, M.D., "Simulation and control of saturated synchronous reluctance machine", *EPE Trondheim*, pp. 3564~3569, 1997.

[7] Franceschini, G., Fratta, A., Petrache, C., and Vagati, A., "Control of high performance synchronous reluctance drives", *Intelligent Motion*, pp. 117~126, June 1994.

[8] Sack, L., "Attributes of servo drive systems with reluctance motors", *EPE Grenoble*, pp. 923~928, 1987.

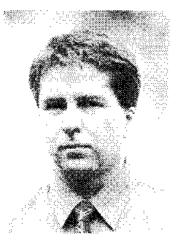

Andreas Kilthau received the Dipl.-Ing. degree in electrical engineering from the University of Darmstadt, Germany, in 1996. He has been with the Institute of Power Electronics and Electrical Drives, Univ. of Siegen, Germany, as a Research Assistant. His research activities are related to the control of synchronous reluctance machines.

José Mario Pacas studied Electrical Eng. at the University of Karlsruhe in Germany obtaining the Dipl.-Ing. and the Dr.-Ing.–degree in 1978 and 1985 respectively. From 1985 to 1995 he worked for BBC/ABB in Switzerland and Germany in different R&D and management positions with a very wide experience in international projects. In the last years with ABB he was responsible for the development of servo drives and later Product Responsible Manager for these products. Since 1995, he is a member of the Faculty of Electrical Engineering and Computer Sciences of the University of Siegen and heads the Institute of Power Electronics and Electrical Drives. Dr. Pacas is technical consultant to some German companies working in the field of high dynamic drives and power electronics. His special fields of interest are motion control, the integration of intelligent power components, optimisation of mechatronic systems and the rational use of electrical energy in industrial environments.